- *脳卒中は救急疾患であり，より早期からの評価と治療が重要である．*
- *急性期虚血性脳血管障害に対する rt-PA 静注療法が承認されて5年が経過した．*
- *承認後調査により rt-PA 静注療法の安全性と有効性が確認された．*

600例を登録し，その治療成績を明らかにした[2]．これは，同時期に国内で rt-PA 静注療法を受けた患者推定数13,500例の4.4%であった．この研究では，画像上の頭蓋内出血は19.8%，36時間以内の症候性頭蓋内出血は3.7%であった．3ヵ月間に6.2%が死亡し，原疾患による直接死が13例，肺炎が6例，心不全が5例を占めた．発症3ヵ月後に39%が完全自立(mRS ≦ 1)した．欧州の市販後調査(SITS-MOST)と同様の解析(80歳を超える高齢者や投与前 NIHSS スコア25以上の重症例を除外)を行うと，43%が3ヵ月後に完全自立であった．多数の脳卒中患者を治療する国内基幹施設における良好な治療成績が明らかとなった．

3. 低用量アルテプラーゼの有効性を確認するための承認後臨床試験

Japan Alteplase Clinical Trial Ⅱ(J-ACT Ⅱ)試験は，中大脳動脈閉塞患者における rt-PA (0.6 mg/kg アルテプラーゼ)静注療法の有効性を臨床転帰，中大脳動脈の閉塞の再開通率から検討したものである[3]．後述する国内使用成績調査とともに，0.6 mg/kg での有効性，安全性を再確認することが厚生労働省から求められたために行われた．発症3時間以内，20歳以上，MRA で中大脳動脈(M1 または M2)閉塞，NIHSS スコア4～22の基準を満たす脳梗塞58例に，治療前，治療後，6時間目，24～36時間目に MRA が実施され，閉塞部位の再開通の有無が検討された．その結果，再開通率は6時間後51.7%，24時間後69.0%と良好であった．3ヵ月後の完全自立(mRS ≦ 1)は46.6%だった．6時間後に再開通した症例の66.7%(非再開通例の25.9%)，24時間後に再開通した症例の62.5%(非再開通例の11.8%)が完全自立であり，いずれの時点でも再開通と完全自立との間に有意な関係があった．多変量解析では，完全自立に独立して関連していたのは，治療前 NIHSS スコア，6時間後までの再開通，24時間後までの再開通，6～24時間に生じる遅発性再開通であった．安全性については，症候性頭蓋内出血はなく，無症候性頭蓋内出血が19.0%に出現した．この試験結果により，0.6 mg/kg でも有効かつ安全に rt-PA 静注療法が行えることが再確認された．

4. 承認後の国内使用成績調査

Japan post-Marketing Alteplase Registration Study (J-MARS)は，承認後2年間にその安全性と有効性を検討するために行われた市販後使用成績調査(全例調査)である[4]．推定使用症例数8,313例中7,692例が登録され，うち有効な調査票を回収した7,492例(97.4%)が解析された．62%が男性で，年齢の中央値は72歳であった．臨床病型では，心原性脳塞栓症が60%と最多であった．副作用報告は2,412件(32.2%)で，治療後36時間以内の頭蓋内出血は16.2%，症候性頭蓋内出血は3.5%，3ヵ月以内の死亡は13.1%(**表1**)，頭蓋内出血を死因とする死亡は0.9%であった．施設あたりの治療症例数が多いほど症候性頭蓋内

- *J-MARSによるとrt-PA静注療法後の症候性頭蓋内出血は3.5%であった.*
- *J-MARSによるとrt-PA静注療法3ヵ月後死亡は13.1%であった.*
- *rt-PA静注療法の安全性は欧米の調査と同程度であった.*

表1　国内外の臨床試験・承認後調査における安全性の比較

	症候性頭蓋内出血* % (95% 信頼区間)	3ヵ月後までの死亡** % (95% 信頼区間)
臨床試験		
無作為割付試験(NINDS, ECASS I-II, ATLANTIS)の実薬群(n＝463)	8.6 (6.3～11.6)	17.3 (14.1～21.1)
J-ACT (日本, n＝103)	5.8	9.7
各国の承認後調査		
J-MARS (日本, n＝7,492)	3.5 (3.1～3.9)	13.1 (12.4～13.9)
SITS-MOST (EU, n＝6,483)	7.3 (6.7～7.9)	11.3 (10.5～12.1)
CASES (カナダ, n＝1,135)	4.6 (3.4～6)	22.3 (20～25)
STARS (米国, n＝389)	3.3 (1.8～5.6)	13★

*「症候性頭蓋内出血」は発症24～36時間後の頭蓋内出血で，NIHSSスコアが1点以上(J-ACTは原則4点以上)の増悪を伴うものを指す
**「3ヵ月後までの死亡」のうち★STARSのみは1ヵ月後までの死亡を示す

出血発生率が低下することがわかった．発症前に完全自立(mRS ≦ 1)であり，かつ3ヵ月後のmRSを評価し得た4,944例の，発症3ヵ月後の完全自立は33%であった(図1)．J-ACTや国外の成績と比べると，3ヵ月後の完全自立はJ-ACT 37%に対してJ-MARS 33%で，死亡はJ-ACT 10%に対してJ-MARS 17%であった．この理由として80歳を超える高齢者や重症例がJ-MARSに多く含まれていたことが考えられた．Standard Treatment with Alteplase to Reverse Stroke (STARS)試験，Canadian Alteplase for Stroke Effectiveness Study (CASES)，Safe Implementation of Thrombolysis in Stroke-Monitoring Study (SITS-MOST)は，おのおの米国，カナダ，EU諸国での市販後調査成績である．特に，SITS-MOSTは6,483例を登録した過去最大規模の調査で，国内成績と比較検討するうえでも大いに参考になる．SITS-MOSTでは，80歳を超える高齢者や投与前NIHSS 25以上の重症例は検討対象から除外しているが，J-MARSに登録された症例から同様の症例を除外した3,576例では完全自立39%，死亡12%となる．これらの市販後調査の結果をおおまかにまとめると，「rt-PA静注療法後の症候性頭蓋内出血は1割未満で，3ヵ月後に約4割の患者が完全自立している一方，1～2割が死の転帰をとる」といえる．

5.　アルテプラーゼ添付文書や適正治療指針の改定

2007年7月25日にアルテプラーゼ添付文書が改定され，胸部大動脈解離あるいは胸部大動脈瘤

- *J-MARS によると rt-PA 静注療法後の 3ヵ月後完全自立は 33% であった.*
- *SITS-MOST(欧州調査)の基準に合わせると3ヵ月後完全自立は39% であった.*
- *rt-PA 静注療法の有効性は欧米の調査と同程度であった.*

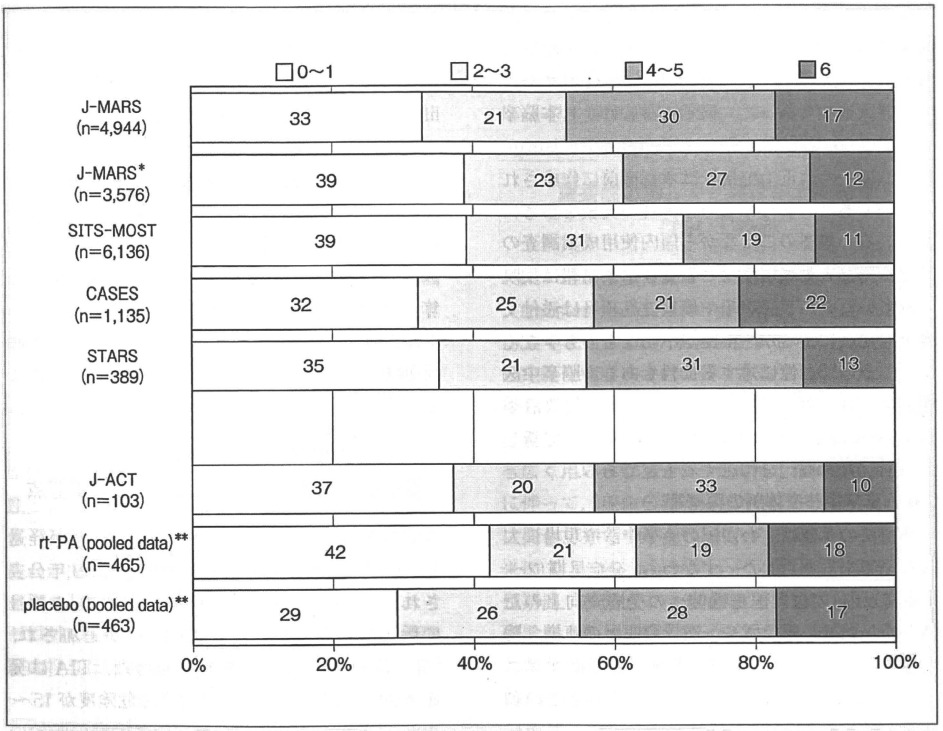

図1　国内外の臨床試験・承認後調査における発症後3ヵ月後の Modified Rankin Scale の比較

Modified Rankin Scale スコアの 0 は「全く症状なし」, 1 は「何らかの症状はあるが障害はない：通常の仕事や活動はすべて行える」, 2 は「軽微な障害：これまでの活動のすべてはできないが身のまわりのことは援助なしでできる」, 3 は「中等度の障害：何らかの援助を要するが援助なしで歩行できる」, 4 は「中等度から重度の障害：援助なしでは歩行できず, 身のまわりのこともできない」, 5 は「重度の障害：ねたきり, 失禁, 全面的な介護」, 6 は「死亡」

*SITS-MOST に合わせて 17 歳以下と 81 歳以上, 治療前 NIHSS スコア 25 以上を除外した

**pooled data は無作為割付試験(NINDS, ECASS Ⅰ-Ⅱ, ATLANTIS)の統合データ

- *J-MARS の結果を踏まえ「rt-PA 静注療法適正治療指針」の改定が予定されている.*
- *rt-PA 静注療法を受ける機会を増やすために脳卒中診療体制の再構築が行われている.*
- *2009 年に脳卒中治療ガイドラインが改定された.*

に関する警告がなされた．これは，胸部大動脈解離や胸部大動脈瘤合併患者に rt-PA 静注療法を施行し，死亡に至った症例が 10 例集積されたことに伴う措置であった．同年 8 月には，日本脳卒中学会も注意喚起を行った(http:/www.jsts.gr.jp/)．現行の適正治療指針は承認直前に作成されたものであり，多くは当時の海外の実績を参考にしている．当然のことながら国内使用成績調査の結果や胸部大動脈解離などの有害事象情報は反映されていない．禁忌事項や慎重投与項目は添付文書上の記載によるが，根拠が不明なものも少なくなく，その妥当性に対する批判もある．脳卒中医療向上・社会保険委員会は「適正治療指針改訂委員会」を組織し，J-MARS の結果を踏まえて新しい「適正治療指針」を作成する予定である．

6. 脳卒中診療体制の再構築

本療法の承認は，わが国の脳卒中診療現場に大きな影響をもたらした．すなわち，発症早期(2～3 時間以内)の専門医療機関への受診率向上のための市民啓発，救急隊や一般診療医との連携，院内脳卒中救急診療体制の再構築，脳卒中ケアユニット(SCU)や脳卒中センターの整備などの動きが盛んになっている．すべての国民が適切に rt-PA 静注療法を受ける機会を与えられるためには，患者が発症 2 時間以内に到着できる範囲内に，24 時間 365 日体制で本療法を実施可能な専門病院(脳卒中センター)が配置され，そのネットワークが構築されるのが理想である．離島やへき地に対しても，遠隔医療支援システム telemedicine の整備などの対策が必要であろう．また，急性期医療のみでなく，病院前救護 prehospital stroke life support (PSLS)や回復期リハビリテーション，慢性期の介護システム，再発予防のための地域医療などとの効果的な連携，すなわち脳卒中地域医療連携の確立を目指す必要がある．診療報酬については，2006 年に「脳卒中ケアユニット入院医療管理料」が，2008 年には「超急性期脳卒中加算」が創設された．いずれも施設要件などのハードルが高すぎるなどの批判もあるが，こうした診療報酬上の重点的な扱いは過去に例のなかったことである．

急性期脳梗塞治療における脳卒中治療ガイドライン 2009 での改訂点

脳卒中治療ガイドライン 2004 から 5 年が経過し，脳卒中治療ガイドライン 2009 が 2009 年公表された[5]．2009 では 2004 の「Ⅱ．脳梗塞」の項目に新たに一過性脳虚血発作(TIA)が追加され，「Ⅱ．脳梗塞・TIA」に変更となった．TIA は発症後 90 日以内に脳卒中を発症する危険度が 15～20% であり，その速やかな評価と治療の開始の重要性が記載された．「脳梗塞急性期治療」における主な改訂点は，rt-PA 静注療法の国内承認に伴う推奨文の改訂，開頭減圧療法の適応の明記，「特殊な病態による脳梗塞の治療」の項への脳動脈解離，大動脈解離，脳静脈・静脈洞閉塞症の追記で

- *脳卒中治療ガイドライン 2009 では rt-PA 静注療法が国内承認に合わせて改訂された.*
- *脳卒中治療ガイドライン 2009 では TIA の速やかな評価と治療の重要性が記載された.*
- *脳卒中治療ガイドライン 2009 では脳梗塞に対する開頭減圧手術の適応が明記された.*

あった. すでに 2004 に rt-PA 静注療法はグレードA(行うよう強く勧められる)として記載されていたが, 当時わが国では虚血性脳血管障害に適応がなかった. 2002 年からアルテプラーゼ(0.6 mg/kg)を用いたオープン試験である国内第Ⅲ相治験 Japan Alteplase Clinical Trial (J-ACT) が行われ, 海外の無作為割付試験の実薬群と同等の有効性と安全性が得られたため, 2005 年 10 月に国内承認された. 本療法の適応決定には除外項目, 慎重投与項目が定められている. 日本脳卒中学会により rt-PA 静注療法実施施設要件が提案, 推奨されている. また, 2008 年 9 月に欧州から European Cooperative Acute Stroke Study Ⅲ (ECASS Ⅲ) の結果が発表され 3～4.5 時間の虚血性脳血管障害に対する rt-PA 静注療法の有効性と安全性が証明された[6]. この成績も, 今回のガイドラインの本文中に紹介された. 一方で, 現在わが国でも DIAS-J として治験中であるデスモテプラーゼは,「現時点において, アルテプラーゼ以外の t-PA, desmoteplase (本邦未承認) の静脈内投与は十分な科学的根拠がなく, 推奨されない(グレード C2 [科学的根拠がないので, 勧められない])」と記載された. 発症 48 時間以内の中大脳動脈灌流域を含む一側大脳半球梗塞のうち, 進行する脳浮腫によって死の転帰をきたす悪性中大脳動脈梗塞 malignant MCA infarction に対する「開頭減圧療法」はグレードAとして推奨された. これは, French DECIMAL, German DENSITY, Dutch HAMLET の統合解析結果を受けたものである.「特殊な病態による脳梗塞の治療」の「大動脈解離」の項で,「大動脈解離を合併する脳梗塞では rt-PA 静注療法は禁忌である[グレードD(行わないよう勧められる)]」ことが記載された.

重要性を増した一過性脳虚血発作(TIA)の診療

1. TIA 概念の変遷

transient ischemic attack (TIA) という名称は, 1951 年に Fisher が最初に記載した. その後 TIA の定義や病態について長く議論されてきた. 1990 年の NINDS 分類では「24 時間以内に消失する, 虚血による一過性の神経症状」とされ, わが国でも広く用いられてきた. しかし, 画像診断の進歩に伴って, 虚血病巣の有無や症状の継続時間などに関していくつかの再検討がなされた. 2002 年, 米国 TIA ワーキンググループは「神経症状がより短期間, 典型的には 1 時間以内に消失し, かつ画像診断上脳梗塞巣が認められないもの」とする新しい TIA の定義を提案し, 2006 年の AHA/ASA「脳梗塞および TIA 患者の再発防止のためのガイドライン」にもこの定義が使用された. 2009 年の AHA/ASA ステートメントでは,「局所の脳, 脊髄, 網膜の虚血により生じる一過性神経学的機能障害で, 画像上脳梗塞巣を伴っていない」ものとした. この声明では, 救急疾患としての TIA と虚血性脳卒中は同一スペクトラム上にあり, 両者

- *脳卒中治療ガイドライン2009では発症4.5時間までのrt-PA静注療法の有効性と安全性も紹介された.*
- *大動脈解離を合併する脳梗塞ではrt-PA静注療法は禁忌である.*
- *TIAを急性期脳梗塞と一緒に急性脳血管症候群(ACVS)と呼ぶことが提唱されている.*

表2 TIAのリスク層別化(ABCD^{2}スコア)

A	Age(年齢)＞60歳(1点)
B	Blood pressure(血圧)＞140/90 mmHg(1点)
C	Clinical feature(臨床像)； 片麻痺(2点)，運動麻痺のない言語障害(1点)
D^2	Diabetes(糖尿病)(1点)および Duration of symptoms(症状の持続時間) (10～59分は1点，60分以上は2点)

(文献8)より改変引用)

を持続時間のみで区別せず，両者を包括する新しい臨床概念として急性脳血管症候群acute cerebrovascular syndrome(ACVS)と呼ぶことが提唱されている.

2. TIA発症後早期診断・治療の有効性

TIA後に発症する脳梗塞の約半数はTIA発症後48時間以内に生じる[8]. TIAを早期に診断し治療を開始することでその転帰が大幅に改善するとの報告が2007年ごろから相ついだ. 英国のEXPRESS研究によれば，TIA発症平均1日後に治療を開始した場合の90日以内の脳卒中発症率は2.1%で，平均20日後に治療を開始した場合に比べて90日以内の脳梗塞発症率が80%軽減し，入院期間の短縮や入院経費，さらに6ヵ月後の後遺症も軽減した[7]. 具体的な治療内容は，スタチン，アスピリンとクロピドグレル併用，降圧薬未投与例への降圧薬，降圧薬2剤使用などであった. フランスのSOS-TIA研究では，1日24時間対応型TIA専門病院で発症24時間以内にTIAあるいは軽症脳卒中と診断し直ちに治療を開始した場合，90日以内の脳卒中発症率は1.24%と低く，治療しなかった場合の発症予測値と比較して79.2%も少なかった. これらの事実に基づき，TIAの早期診断・治療が重視されるようになった. 現在，国際共同研究によりTIA患者を多数登録し，長期間前向きに追跡調査して脳卒中などの心血管イベントの発症リスクを解析するとともに，各国における診断と治療の実態を明らかにしようとする疾患コホート研究(TIAregistry.org)が進行中であり，当センターを含む国内数施設も登録に参加している.

3. TIA発症後早期の脳卒中発症に関する予測因子

TIA発症後早期の脳卒中リスクを予測するABCD^{2}スコア(表2)[8]を用いたTIA診療を一般診療医に啓発する活動が展開されている. ABCD^{2}スコアは，A(age)，B(blood pressure)，C(clinical features)，D(duration of symptoms)およびD(diabetes)の頭文字を示すものであり，各項目の合計点で脳卒中の発症リスクを評価する. TIA発症後48時間以内の脳卒中リスクは，ABCD^{2}スコアが0～3点では1.0%，4～5点では4.1%，6～7点では8.1%で，その点数が高いほど脳卒中発症リスクは高い. 頭部MRI検査によるDWI陽性所見の有無，大血管動脈硬化病変の有無をABCD^{2}スコアに加えることによりTIA後早期の脳卒中発症リスクの予測精度をさらに高めること

- *TIA を速やかに評価・治療することで90日以内の脳梗塞発症は8割減る.*
- *TIA 発症後早期の脳卒中リスク予測には $ABCD^2$ スコアが有用である.*
- *$ABCD^2$ スコアに DWI 所見などを加えると脳卒中発症リスクの予測精度が高まる.*

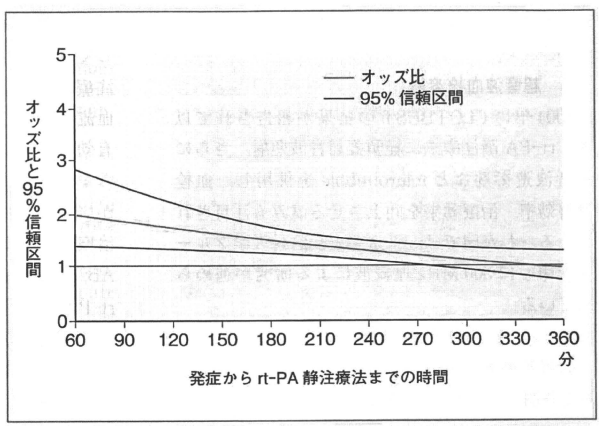

図2　rt-PA 静注療法無作為割付試験の統合解析による3ヵ月後完全自立のオッズ比
(文献9)より改変引用)

ができる.

新しい超急性期治療の追求

1. 発症後3～4.5時間の rt-PA 静注療法

2004年に NINDS-1, NINDS-2, ATLANTIS, ECASS, ECASS Ⅱの統合解析結果が報告されたが, 最近, 発症3時間以降を対象とした ECASS Ⅲと EPITHET を加えた rt-PA 静注療法の有効性と安全性の再検討結果が報告された[9]. この研究では, 発症から治療開始までの時間(OTT)と, 3ヵ月後完全自立(mRS ≦ 1), 3ヵ月以内死亡, 症候性頭蓋内出血との関連が解析された. rt-PA を受けた患者では完全自立の補正オッズ比が OTT 1.5時間以内で2.55(95% 信頼区間1.44～4.52), 1.5～3時間で1.64(1.12～2.40), 3～4.5時間で1.34(1.06～1.68), 4.5～6時 間 で1.22(0.92～1.61)で, 4.5時間までは rt-PA 群で完全自立が有意に多く, 4.5～6時間では差が消失した(図2). 死亡は4.5時間以降に増加する傾向があった. 症候性頭蓋内出血と OTT に有意な関連はなかった. これらの結果を受けて豪州ではすでに添付文書の改訂が行われ, 発症後4.5時間までを rt-PA 静注療法の対象としている. 欧米やわが国でも添付文書の改訂に向けた検討が行われている. たとえ, 治療可能時間が4.5時間までに延長されたとしても rt-PA 静注療法の効果を最大限にするた

- *RCT 統合解析結果によると rt-PA 静注療法により発症 4.5 時間まで完全自立が多い.*
- *RCT 統合解析結果によると rt-PA 静注療法により発症 4.5 時間以降に死亡が増える.*
- *rt-PA 静注療法の効果を最大限にするためにはより早期に治療を開始すべきである.*
- *急性期脳梗塞の新規治療として超音波血栓溶解療法が注目されている.*
- *デスモテプラーゼの発症 9 時間までの治療効果を評価中である.*
- *Merci や Penumbra といった血管内血栓回収デバイスが注目されている.*

めに OTT を短縮するための努力を忘れてはならない.

2. 超音波血栓溶解

2004 年に CLOTBUST の結果が報告されて以来, rt-PA 静注療法に経頭蓋超音波照射, さらに超音波造影剤など microbubble を併用し, 血栓溶解効率, 治療効果を向上させる試みも注目されている. わが国では, 東京慈恵会医科大学グループを中心に 500 MHz 連続波による研究が進められている.

3. デスモテプラーゼ治療

血栓溶解薬の投与可能時間を延長する可能性のある薬剤として第三世代血栓溶解薬デスモテプラーゼがある. MRI の diffusion-perfusion mismatch でペナンブラ領域が検出された発症 3～9 時間の患者を対象に無作為割付試験が実施された. 第Ⅱ相試験では用量依存性の治療効果が示唆されたが, 第Ⅲ相試験では明らかな治療効果は示されなかった. 本薬については選択基準などを変更した新しい国際共同の第Ⅲ相試験が, わが国でも独自の第Ⅱ相試験(DIAS-J)が行われている.

4. 血管内治療デバイス

主幹脳動脈閉塞による急性期脳梗塞に対する血栓回収を目的とした血管内治療デバイスが登場してきた. わが国では 2010 年 4 月に Merci リトリーバーが承認された. 米国の試験では, 発症 8 時間以内の主幹動脈閉塞脳梗塞例の 68% で再開通が得られ, 症候性頭蓋内出血が 9.8% で, 再開通例では転帰が改善した. わが国での適応は, 原則として発症 8 時間以内の急性期脳梗塞で, rt-PA 静注療法の適応外, または rt-PA 静注療法により血流再開が得られなかった患者である. 本療法の有効性および安全性は, まだ十分に確認されておらず, 市販後調査やその他の臨床研究により明らかにされるべきであろう. ほかに, 有望な血管内治療デバイスとして Penumbra システムや Solitare AB, Trevo などがある. 現在, 発症 3 時間以内の rt-PA 静注療法とその後の血管内局所線溶や血管内血栓摘除術などとの併用効果を調べる無作為割付試験である Interventional Management of Stroke (IMS) Trial Ⅲが進行中である.

おわりに

rt-PA 静注療法により脳卒中診療体制の再構築が進行中である. さらに多くの脳卒中患者が本療法の恩恵に与るためには, 一般市民への啓発, 救急隊との密な連携, それぞれの地域での脳卒中診療体制の整備が必須である. 新規の血管内治療デバイスなど beyond rt-PA への取り組みも本格化しており, 今後は rt-PA 静注療法の限界を超える安全かつ有効な脳卒中治療法の確立が期待される.

文 献

1) Nakashima, T. et al.: Arterial occlusion sites on MRA influence the efficacy of intravenous low-

dose (0.6 mg/kg) alteplase therapy for ischemic stroke. Int J Stroke 4 : 425-431, 2007
2) Toyoda, K. et al. : Routine use of intravenous low-dose recombinant tissue plasminogen activator in Japanese patients. Stroke **40** : 3591-3595, 2009
3) Mori, E. et al. : Effects of 0.6 mg/kg intravenous alteplase on vascular and clinical outcomes in middle cerebral artery occlusion : Japan Alteplase Clinical Trial Ⅱ (J-ACT Ⅱ). Stroke **41** : 461-465, 2010
4) Nakagawara, J. et al. : Thrombolysis with 0.6 mg/kg intravenous alteplase for acute ischemic stroke in routine clinical practice : the Japan post-Marketing Alteplase Registration Study (J-MARS). Stroke **41** : 1984-1989, 2010
5) 篠原幸人ほか：脳卒中治療ガイドライン 2009, 協和企画, 東京, 2009
6) Hacke, W. et al. : Thrombolysis with alteplase 3 to 4.5 hours after acute ischemic stroke. N Engl J Med **359** : 1317-1329, 2008
7) Rothwell, P.M. et al. : Effect of urgent treatment of transient ischaemic attack and minor stroke on early recurrent stroke (EXPRESS study) : a prospective population-based sequential comparison. Lancet **370** : 1432-1442, 2007
8) Johnston, S.C. et al. : Validation and refinement of scores to predict very early stroke risk after transient ischaemic attack. Lancet **369** : 283-292, 2007
9) Lees, K.R. et al. : Time to treatment with intravenous alteplase and outcome in stroke : an updated pooled analysis of ECASS, ATLANTIS, NINDS, and EPITHET trials. Lancet **375** : 1695-1703, 2010

Carotid Duplex Ultrasonography Can Predict Outcome of Intravenous Alteplase Therapy for Hyperacute Stroke

Masatoshi Koga, MD, Kazunori Toyoda, MD, Takahiro Nakashima, MD, Boo-Han Hyun, MD, Toshiyuki Uehara, MD, Chiaki Yokota, MD, Kazuyuki Nagatsuka, MD, Hiroaki Naritomi, MD, and Kazuo Minematsu, MD

We evaluated whether carotid duplex ultrasonography (US) can help predict the safety and efficacy of treating hyperacute stroke with intravenous (IV) tissue plasminogen activator (alteplase) therapy. Consecutive patients with stroke were assigned to the carotid artery occlusion (CO) group or the other (non-CO) group according to US findings before or immediately after receiving IV alteplase. Effectiveness and safety outcomes included early neurologic improvement, defined as a reduction in a National Institutes of Health Stroke Scale (NIHSS) score of ≥4 points within the initial 24 hours after stroke onset; completely independent routine activity, defined as a modified Rankin Scale score of ≤1 at day 90 after stroke onset; symptomatic intracranial hemorrhage (ICH) occurring within 36 hours after stroke onset; and any ICH. We enrolled 127 patients (27 in the CO group and 100 in the non-CO group) with a median baseline NIHSS score of 13 (range, 4-30). The CO group had a higher baseline NIHSS score (median, 18 vs 12; $P = .005$). After multivariate adjustment, the CO group was inversely associated with early improvement (odds ratio [OR] = 0.26; 95% confidence interval [CI] = 0.09-0.72) and independence at day 90 (OR = 0.23; 95% CI = 0.05-0.73) and positively associated with any ICH (OR = 3.11; 95% CI = 1.23-8.48). Our findings indicate that CO identified by US in the emergency clinical setting is an independent predictor of unfavorable outcome and ICH following IV alteplase therapy. **Key Words:** Alteplase—internal carotid artery occlusion—intracranial hemorrhage—ultrasonography—outcome.

Occlusion of the internal carotid artery (ICA) often provokes severe hypoperfusion of cerebral blood flow in the affected territory. Patients who sustain acute ICA occlusion tend to have poor clinical outcomes.[1] Mortality is high in patients with malignant middle cerebral artery (MCA) infarction, resulting principally from distal ICA occlusion. The fates of patients with and without a major arterial occlusive lesion might differ after intravenous (IV) tissue plasminogen activator (alteplase) therapy, because resistance to clot lysis and the fragility of infarcted brain tissue may depend on the patency of the ICA. Rapid evaluation of arterial status in the emergency clinical setting may help predict outcome after alteplase therapy.

Magnetic resonance angiography (MRA) and computed tomographic angiography (CTA) can detect occlusions or severe stenoses of the cervicocephalic arteries supplying the infarcted area in patients with acute stroke,[2,3] as well as intracranial abnormalities with greater sensitivity and specificity, than conventional cerebral angiography.[3,4] Large ischemic lesions on diffusion magnetic resonance

From the Cerebrovascular Division, Department of Medicine, National Cardiovascular Center, Suita, Osaka, Japan.

Received August 17, 2009; revision received September 25, 2009; accepted October 2, 2009.

Supported in part by a Grant-in-Aid (H20-Junkanki-Ippan-019) from the Ministry of Health, Labor, and Welfare of Japan.

Address correspondence to Masatoshi Koga, MD, Cerebrovascular Division, National Cardiovascular Center, 5-7-1 Fujishirodai, Suita, Osaka 565-8565, Japan. E-mail: koga@hsp.ncvc.go.jp.

1052-3057/$ - see front matter

doi:10.1016/j.jstrokecerebrovasdis.2009.10.003

imaging (MRI) before IV alteplase therapy predict poor outcome in patients with acute ischemic stroke,[5] and diffusion–perfusion mismatch can select patients with remaining salvageable tissue.[6] But MRI takes at least 15 minutes, including equipment arrangement and patient transfer, to generate information, and CTA carries a risk of renal failure and anaphylaxis.

Carotid duplex ultrasonography (US) is another noninvasive tool that can detect major extracranial carotid arterial disease.[7-10] Compared with conventional cerebral angiography, US is not associated with such invasive complications as cerebral and systemic embolism, contrast agent anaphylaxis, acute renal dysfunction, and arterial dissection.[11] Morever, with bedside US, it takes only a few minutes to detect significant occlusive lesions of carotid arteries. US findings can help identify the mechanism and type of ischemic stroke.

We tested the hypothesis that carotid duplex US findings can help predict the outcome and safety of IV alteplase therapy for patients with hyperacute ischemic stroke.

Materials and Methods

We prospectively enrolled all patients with stroke who were admitted to our emergency stroke care unit and received IV alteplase therapy between October 2005 (when this therapy was approved in Japan) and July 2008. Our institution's Ethics Committee approved the research protocol. Patients or their representatives (eg, family members) provided written informed consent for the treatment.

Patient eligibility for IV alteplase therapy was based principally on the inclusion and exclusion criteria applied in the National Institute of Neurological Disorders and Stroke (NINDS) study[12] and in the Japan Alteplase Clinical Trial (J-ACT).[13] Each patient received a single IV dose of 0.6 mg/kg (not exceeding 60 mg) of alteplase, with 10% given as a bolus, followed by a continuous IV infusion of the remainder over 1 hour, in accordance with the Japanese guidelines for IV alteplase therapy based on the J-ACT results.[13,14] As in the NINDS study,[12] the use of antithrombotic agents were prohibited for 24 hours after onset, blood pressure was maintained at <180/105 mm Hg, and neurologic symptoms were monitored.

Clinical data included age and sex; time from symptom onset (or time when the patient last appeared to be normal) to the initiation of IV alteplase therapy; carotid artery US findings before or immediately after the initiation of alteplase therapy; National Institute of Health Stroke Scale (NIHSS) score immediately before (baseline) and 24 hours after alteplase therapy; concomitant diseases; current smoking and drinking habits; imaging data, including hemorrhagic transformation detected by computed tomography (CT) or MRI during hospitalization; stroke subtype according to Trial of Org 10172 in Acute Stroke Treatment (TOAST) criteria;[15] and modified Rankin Scale (mRS) score at day 90. Among concomitant diseases, hypertension was defined as systolic blood pressure ≥140 mm Hg or diastolic blood pressure ≥90 mm Hg before stroke onset or the use of antihypertensive medication. Diabetes was defined as preceding fasting blood glucose ≥126 mg/dL or the use of oral antidiabetic agents or insulin. Hypercholesterolemia was defined as total plasma cholesterol level ≥220 mg/dL or the use of antihypercholesterolemic medication.

Patients underwent US after hospitalization while awaiting the results of blood tests or immediately after starting alteplase therapy. US was performed with a bedside unit (Sonos 5500; Philips Medical Systems, Tokyo, Japan) with a 3- to 11-MHz linear transducer. On US, absent color flow signals on the ICA indicates the occlusion at or proximal to the artery, and absent end-diastolic flow velocity of the ICA indicates intracranial ICA occlusion.[16] Thus, carotid artery occlusion was defined as either of these US findings (Fig 1). Based on the US findings, the patients were divided into 2 groups: those with carotid artery occlusion (designated the CO group) and those without carotid artery occlusion (designated the non-CO group).

Before alteplase therapy, all patients underwent intracranial MRA to serve as the gold standard reference of carotid US findings, unless contraindicated. MRA was performed using the 3-dimensional time-of-flight technique (repetition time/echo time, 35/7.2 msec; 20-degree flip angle) with a 1.5 T system (Magnetom Vision; Siemens, Germany).

Outcomes included early neurologic improvement, defined as a ≥4-point reduction in NIHSS score within the initial 24 hours, and complete independence in activities of daily living (ADL), defined as an mRS score of 0 or 1, at 90 days. To assess long-term independence, patients with a mRS score of ≥2 before stroke onset were excluded. Safety outcomes included any intracranial hemorrhage (ICH) confirmed by head CT or MRI during hospitalization, and symptomatic ICH defined as early ICH with neurologic deterioration corresponding to a ≥1-point increase in the NIHSS score within 36 hours after alteplase therapy.

Statistical Analysis

Sensitivity, specificity, positive predictive value, and negative predictive value for detectng patients with carotid artery occlusion by carotid US were calculated when intracranial MRA findings were used as gold standard. Continuous and categorized variables were compared using the Student *t*-test and the χ^2 test, respectively. Nonparametric independent group comparisons were done using the Mann-Whitney *U*-test. To determine independent clinical variables to predict outcomes, significant variables were analyzed in a logistic regression model, with multivariate adjustments for age, sex, and confounders with an association of $P < .05$ with each outcome in univariate analysis. Statistical significance was established at $P < .05$.

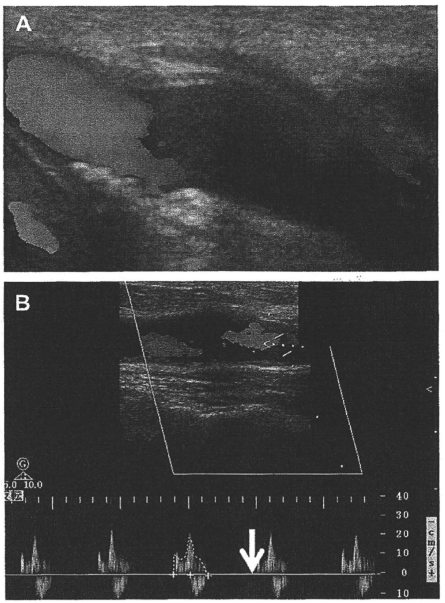

Figure 1. *Typical carotid US findings in ICA occlusion. (A) Absent flow of color in the affected ICA origin in a patient with atherothrombotic extracranial ICA occlusion. (B) Absent end-diastolic flow velocity of affected ICA (arrow) detected by pulsed Doppler US in a patient with distal ICA occlusion.*

Results

A total of 127 patients (89 men, mean age, 73 ± 9 years) were enrolled in the study. In 27 patients, carotid artery occlusion was detected by carotid US before or immediately after alteplase therapy. A total of 110 patients (87%) underwent MRA; 23 were found to have ICA occlusion. Sensitivity, specificity, positive predictive value, and negative predictive value for detect carotid artery occlusion by carotid US were 96%, 97%, 88%, and 99%, respectively. Table 1 summarizes the baseline characteristics and clinical outcomes of the study population. The median baseline NIHSS score was 13 (range, 4-30) and was higher in the CO group than in the non-CO group ($P = .005$). The median duration from symptom onset to IV alteplase therapy was 135 min (range, 50-180 min). US found no evidence of common carotid artery dissection possibly extending from the aortic arch in any patient. This finding, in combination with later examinations, ruled out aortic dissection in all patients.

Cardioembolism was the leading stroke subtype (57%). Atrial fibrillation was more common in the CO group than in the non-CO group. Early neurologic improvement and independence at day 90 were apparently less frequent in the CO group, whereas any ICH was more frequent in the CO group. Two patients in the CO group (7.4%) died within 90 days, one of symptomatic ICH and the other (who had asymptomatic ICH) of severe cerebral herniation due to massive stroke.

We used univariate analysis to test associations of the characteristic variables listed in Table 1 with outcomes (Table 2). Baseline NIHSS ($P = .042$), diabetes mellitus ($P = .049$), and carotid artery occlusion ($P = .039$) were inversely associated with early neurologic improvement. High pretreatment NIHSS score ($P = .015$) and carotid artery occlusion ($P = .002$) were inversely associated with independence at day 90. High baseline NIHSS score ($P = .047$) and carotid artery occlusion ($P = .009$) were associated with any ICH. No variables were significantly associated with symptomatic ICH.

We analyzed the contributing factors to the efficacy and safety outcomes using multivariate adjustment (Table 3). The CO group was independently associated with the absence of early neurologic improvement (odds ratio [OR] = 3.79; 95% confidence interval [CI] = 1.39-11.42; $P = .008$), absence of complete independence at day 90 (mRS score of ≥2: OR = 4.44; 95% CI = 1.38-19.96; $P = .011$), and presence of ICH (OR = 3.11; 95% CI = 1.23-8.48; $P = .016$). Diabetes mellitus (OR = 2.77; 95% CI = 1.03-8.15; $P = .043$) and low NIHSS score (OR = 1.09; 95% CI = 1.02-1.18 per 1-point decrease; $P = .011$) were associated with the absence of early neurologic improvement.

Discussion

Our data indicate that the likelihood of a good outcome was decreased and the likelihood of ICH was increased in stroke patients with US-identified ICA occlusion after IV alteplase therapy. Rapid evaluation using US thus helped predict the effectiveness and safety of alteplase therapy.

Sites of arterial occlusion before alteplase therapy have frequently been identified using transcranial Doppler (TCD) sonography. Recanalization of the ICA after IV alteplase therapy documented on TCD or angiography is reportedly complete in 10% of patients, partial in 16%, and absent in 74%.[17] In addition, terminal ICA occlusion has the least likelihood of recanalization compared with the other types of occlusion (OR = 0.1).[18] Linfante et al[19] found that patients with ICA occlusion have higher NIHSS scores on days 1 and 3 and a lower proportion of recanalization defined by TCD or MRA compared with those with MCA occlusion after alteplase therapy. Consequently, occlusions at the terminal ICA and at a tandem lesion of the ICA and MCA are predictive of poor outcome after alteplase therapy.[18,20] On the other hand, whether carotid US can detect ICA occlusion in the clinical setting of alteplase therapy has not been unequivocally established.

We used carotid US to evaluate the major cerebral arteries because Asian patients with stroke generally do

Table 1. *Baseline characteristics and clinical outcomes*

		US findings	
	Total (n = 127)	CO group (n = 27)	Non-CO group (n = 100)
Characteristic variables			
Female sex	38 (30)	8 (30)	30 (30)
Age, years	73 ± 9	75 ± 8	73 ± 10
Baseline NIHSS score	13 (4-30)	18 (5-24)	12 (4-30)§
Onset to treatment, minutes	135 (50-180)	130 (79-180)	135.5 (50-180)
Hypertension	80 (64)	21 (78)	59 (59)
Diabetes mellitus	24 (19)	5 (19)	19 (19)
Hypercholesterolemia	34 (27)	7 (26)	27 (27)
Atrial fibrillation	58 (46)	17 (63)	41 (41)‡
Current smoking	31 (25)	8 (30)	23 (23)
Alcohol	59 (47)	14 (52)	45 (45)
Stroke subtype			
Large vessel	21 (17)	7 (26)	14 (14)
Cardioembolic	72 (57)	16 (59)	56 (56)
Small vessel	2 (2)	0 (0)	2 (2)
Other	32 (26)	4 (15)	28 (28)
Outcome variables			
Early neurologic improvement*	60 (47)	8 (30)	52 (52)‡
mRS score at 3 months	3 (0-6)	4 (0-6)	2 (0-6)§
Complete independence at 3 months†	44 (35)	3 (11)	41 (41)§
Any intracranial hemorrhage	61 (48)	19 (70)	42 (42)§
Symptomatic intracranial hemorrhage	5 (4)	1 (4)	4 (4)

Values are mean ± standard deviation in age, median (range) in baseline NIHSS score, interval between onset and treatment and mRS score at 3 months, or number (%) in the remaining variables.

*Reduction in NIHSS score of ≥4 points within the initial 24 hours.

†Defined as a mRS score of 0 or 1. Eleven patients with a score ≥2 before stroke onset were excluded.

‡$P < .05$.

§$P < .01$.

not have a sufficient bone window for TCD,[21,22] and obtaining information about arterial occlusion from TCD can be difficult. As an alternative, carotid US can detect intracranial ICA occlusion based on the absence of end-diastolic flow velocity.[16] The accuracy of the diagnosis of carotid occlusion by US is sufficiently high compared with MRA findings. B-mode, color Doppler, and pulsed-wave Doppler carotid US can identify an ICA occlusion in about 5 minutes. The American Heart and Stroke Association recommends completing the initial evaluation and starting medical therapy within 60 minutes of the patient's arrival at the emergency department.[23] Head CT and bedside carotid US imaging can be completed at the emergency department within the 20 minutes or so needed to generate the results of blood tests, including serum chemistry and hemostatic parameters, at our institute.

Another reason for the routine use of carotid US is to rule out aortic dissection extending to the CCA. Concomitant aortic dissection is a conspicuous cause of in-hospital death following IV alteplase therapy in Japan (Japan Stroke Society; http://www.jsts.gr.jp [in Japanese]).

The present study has some limitations. Carotid US cannot provide information about tandem lesions. The incidence of symptomatic ICH was too low to enable an assessment of its relationship with carotid US findings.

In summary, carotid US is a simple tool for detecting ICA occlusion within a few minutes in the emergency clinical setting of hyperacute stroke. Patients with ICA occlusion according to carotid US had worse outcomes and more ICH after IV alteplase therapy. Therefore, rapid non-invasive evaluation of the carotid artery using US might improve the selection of patients likely to benefit from IV alteplase therapy. Although ICA occlusion is a pessimistic sign for success in IV alteplase therapy, patients with such a lesion may still be candidates for this therapy until an alternative therapeutic strategy is established. In the near future, endovascular thrombus retrieval and

Table 2. *Univariate analysis of outcomes*

	Early neurologic improvement*		Complete independence at day 90†		Any ICH		Symptomatic intracranial hemorrhage	
	Present (n = 60)	Absent (n = 67)	Present (n = 44)	Absent (n = 83)	Present (n = 61)	Absent (n = 66)	Present (n = 5)	Absent (n = 122)
Females	19 (32)	19 (28)	11 (25)	27 (33)	20 (33)	18 (27)	2 (40)	36 (30)
Age, years	72 ± 9	75 ± 9	71 ± 8	74 ± 10	72 ± 9	74 ± 10	78 ± 8	73 ± 10
Baseline NIHSS score	13 (5-30)	11 (4-24)‡	11 (4-30)	13 (4-26)‡	14 (4-24)	11 (4-30)‡	15 (12-21)	12 (4-30)
Onset to treatment time	127.5 (50-180)	140 (78-178)	133.5 (50-180)	139 (78-180)	139 (79-180)	133.5 (50-180)	120 (105-143)	136.5 (50-180)
Hypertension	36 (61)	44 (67)	27 (61)	53 (65)	38 (62)	42 (64)	4 (80)	76 (63)
Diabetes mellitus	7 (12)	17 (25)‡	6 (14)	18 (22)	14 (23)	10 (15)	0 (0)	24 (20)
Hyperlipidemia	16 (27)	18 (27)	11 (25)	23 (28)	13 (21)	21 (32)	0 (0)	34 (28)
Atrial fibrillation	26 (44)	32 (48)	16 (36)	42 (51)	30 (49)	28 (42)	4 (80)	54 (45)
Current smoking	10 (17)	21 (31)	9 (21)	22 (27)	16 (26)	15 (23)	1 (20)	30 (25)
Alcohol consumption	30 (51)	29 (43)	22 (51)	37 (45)	28 (46)	31 (47)	1 (20)	58 (48)
Cardioembolic (subtype)	37 (62)	35 (52)	23 (52)	49 (59)	38 (62)	34 (52)	5 (100)	67 (55)
CO group	8 (13)	19 (28)‡	3 (7)	24 (29)§	19 (31)	8 (12)§	1 (20)	26 (21)

Values are mean ± standard deviation in age, median (range) in baseline NIHSS score, and interval between onset and treatment time, or number (%).
*Reduction in NIHSS score of ≥4 points within the initial 24 hours.
†Defined as mRS score of 0 or 1. Eleven patients with a score of ≥2 before stroke onset were excluded.
‡$P < .05$.
§$P < .01$.

Table 3. *Multivariate analysis of outcomes*

	Absence of early neurologic improvement*			mRS score ≥2 at day 90			Any ICH		
	OR	95% CI	*P*	OR	95% CI	*P*	OR	95% CI	*P*
CO group	3.79	1.39-11.42	.008	4.44	1.38-19.96	.011	3.11	1.23-8.48	.016
Diabetes mellitus	2.77	1.03-8.15	.043	–	–	–	–	–	–
Baseline NIHSS score (per 1-point increase)	0.91	0.85-0.98	.011	1.05	0.98-1.13	.144	1.05	0.98-1.12	.165

Adjusted for age, sex, and confounders with an association of $P < .05$ with each outcome in univariate analysis.
Symptomatic intracranial hemorrhage was not tested due to the absence of significantly associated variables in univariate analysis.
*Increase, no change, or decrease in NIHSS score of <4 points within the initial 24 hours.

sonothrombolysis may improve the outcomes of patients with ICA occlusion, at which point this quick screening using US will work well.

References

1. Paciaroni M, Caso V, Venti M, et al. Outcome in patients with stroke associated with internal carotid artery occlusion. Cerebrovasc Dis 2005;20:108-113.
2. Warach S, Li W, Ronthal M, et al. Acute cerebral ischemia: Evaluation with dynamic contrast-enhanced MR imaging and MR angiography. Radiology 1992;182:41-47.
3. Koelemay MJ, Nederkoorn PJ, Reitsma JB, et al. Systematic review of computed tomographic angiography for assessment of carotid artery disease. Stroke 2004;35:2306-2312.
4. Riles TS, Eidelman EM, Litt AW, et al. Comparison of magnetic resonance angiography, conventional angiography, and duplex scanning. Stroke 1992;23:341-346.
5. Kimura K, Iguchi Y, Shibazaki K, et al. Large ischemic lesions on diffusion-weighted imaging done before intravenous tissue plasminogen activator thrombolysis predicts a poor outcome in patients with acute stroke. Stroke 2008;39:2388-2391.
6. Albers GW. Expanding the window for thrombolytic therapy in acute stroke: The potential role of acute MRI for patient selection. Stroke 1999;30:2230-2237.
7. Wetzner SM, Kiser LC, Bezreh JS. Duplex ultrasound imaging: vascular applications. Radiology 1984;150:507-514.
8. Polak JF, Dobkin GR, O'Leary DH, et al. Internal carotid artery stenosis: accuracy and reproducibility of color Doppler–assisted duplex imaging. Radiology 1989;173:793-798.
9. Steinke W, Kloetzsch C, Hennerici M. Carotid artery disease assessed by color Doppler flow imaging: Correlation with standard Doppler sonography and angiography. AJNR Am J Neuroradiol 1990;11:259-266.
10. Mansour MA, Mattos MA, Hood DB, et al. Detection of total occlusion, string sign, and preocclusive stenosis of the internal carotid artery by color-flow duplex scanning. Am J Surg 1995;170:154-158.
11. Waugh JR, Sacharias N. Arteriographic complications in the DSA era. Radiology 1992;182:243-246.
12. National Institute of Neurological Disorders and Stroke rt-PA Stroke Study Group. Tissue plasminogen activator for acute ischemic stroke. N Engl J Med 1995;333:1581-1587.
13. Yamaguchi T, Mori E, Minematsu K, et al. Alteplase at 0.6 mg/kg for acute ischemic stroke within 3 hours of onset: Japan Alteplase Clinical Trial (J-ACT). Stroke 2006; 37:1810-1815.
14. Shinohara Y, Yamaguchi T. Outline of the Japanese Guidelines for the Management of Stroke 2004 and subsequent revision. Int J Stroke 2008;3:55-62.
15. Adams HP Jr, Bendixen BH, Kappelle LJ, et al. Classification of subtype of acute ischemic stroke: Definitions for use in a multicenter clinical trial. Trial of Org 10172 in Acute Stroke Treatment (TOAST). Stroke 1993;24:35-41.
16. Hoshino H, Takagi M, Takeuchi I, et al. Recanalization of intracranial carotid occlusion detected by duplex carotid sonography. Stroke 1989;20:680-686.
17. Christou I, Felberg RA, Demchuk AM, et al. Intravenous tissue plasminogen activator and flow improvement in acute ischemic stroke patients with internal carotid artery occlusion. J Neuroimaging 2002;12:119-123.
18. Saqqur M, Uchino K, Demchuk AM, et al. Site of arterial occlusion identified by transcranial Doppler predicts the response to intravenous thrombolysis for stroke. Stroke 2007;38:948-954.
19. Linfante I, Llinas RH, Selim M, et al. Clinical and vascular outcome in internal carotid artery versus middle cerebral artery occlusions after intravenous tissue plasminogen activator. Stroke 2002;33:2066-2071.
20. Rubiera M, Ribo M, Delgado-Mederos R, et al. Tandem internal carotid artery/middle cerebral artery occlusion: An independent predictor of poor outcome after systemic thrombolysis. Stroke 2006;37:2301-2305.
21. Itoh T, Matsumoto M, Handa N, et al. Rate of successful recording of blood flow signals in the middle cerebral artery using transcranial Doppler sonography. Stroke 1993;24:1192-1195.
22. Yagita Y, Etani H, Handa N, et al. Effect of transcranial Doppler intensity on successful recording in Japanese patients. Ultrasound Med Biol 1996;22:701-705.
23. Adams HP Jr, del Zoppo G, Alberts MJ, et al. Guidelines for the early management of adults with ischemic stroke: A guideline from the American Heart Association/American Stroke Association Stroke Council, Clinical Cardiology Council, Cardiovascular Radiology and Intervention Council, and the Atherosclerotic Peripheral Vascular Disease and Quality of Care Outcomes in Research Interdisciplinary Working Groups. Stroke 2007;38:1655-1711.

Dual-Frequency Ultrasound Imaging and Therapeutic Bilaminar Array Using Frequency Selective Isolation Layer

Takashi Azuma, Makoto Ogihara, Jun Kubota, *Member, IEEE*, Akira Sasaki, Shin-ichiro Umemura, *Fellow, IEEE*, and Hiroshi Furuhata

Abstract **—A new ultrasound array transducer with two different optimal frequencies designed for diagnosis and therapy integration in Doppler imaging-based transcranial sonothrombolysis is described. Previous studies have shown that respective frequencies around 0.5 and 2 MHz are suitable for sonothrombolysis and Doppler imaging. Because of the small acoustic window available for transcranial ultrasound exposure, it is highly desirable that both therapeutic and diagnostic ultrasounds pass through the same aperture with high efficiency. To achieve such a dual-frequency array transducer, we propose a bilaminar array, having an array for imaging and another for therapy, with a frequency selective isolation layer between the two arrays. The function of this layer is to isolate the imaging array from the therapy array at 2 MHz without disturbing the 0.5-MHz ultrasound transmission. In this study, we first used a 1-D model including two lead zirconate titanate (PZT) layers separated by an isolation layer for intuitive understanding of the phenomena. After that, we optimized the acoustic impedance and thickness of the isolation layer by analyzing pulse propagation in a 2-D model by conducting a numerical simulation with commercially available software. The optimal acoustic impedance and thickness are 3 to 4 MRayl and $\lambda/10$, respectively. On the basis of the optimization, a prototype array transducer was fabricated, and the spatial resolutions of the Doppler images it obtained were found to be practically the same as those obtained through conventional imaging array transducers.**

I. Introduction

Dissolution of a thrombus as soon as possible after an ischemic stroke, typically within three hours, is crucial for reducing the risk of ischemic neuronal injury. Several studies have reported that ultrasound can enhance the effect of thrombolytic drugs such as tissue plasminogen activator (tPA) and urokinase. Alexandrov *et al.* found that a significantly higher rate of recanalization with tPA was observed in acute ischemic stroke patients who were monitored with a transcranial Doppler (TCD) at 2 MHz than in those who were not, and they concluded that ultrasound including TCD could enhance the thrombolytic activity of tPA [1]. Several other groups have also reported similar effects [2]–[4].

Adverse effects caused by ultrasound can be mechanical or thermal. Mechanical effects are caused by the creation and rupture of ultrasound-induced microbubbles through cavitation. Several groups suggested that these mechanical effects caused adverse effects in clinical cases [5]–[7]. Because standing wave generation in the cranium can increase the risk of adverse effects caused by cavitation, suppressing mechanical effects in the cranium is important [8], [9]. A mechanical index is generally used to assess the risk of this effect occurring, and it is inversely proportional to the square root of the frequency.

Thermal effects are also caused by ultrasound absorption in tissue. A thermal index is the standard index of thermal effects and is approximately proportional to the frequency. To avoid a temperature rise caused by absorption during propagation of ultrasound in the cranium, it is important to avoid using any high attenuation areas in the cranium as an acoustic aperture. The cranium typically has a diploe layer, which is a sponge-like layer containing many pores a few hundred micrometers in diameter. Although this diploe layer produces such strong scattering that the propagation of ultrasound through the diploe is disturbed, most skulls have a thinner diploe layer or none at all in the temple area. Previous studies showed that transmittances without diploe at frequencies of 0.5 and 2 MHz are 6 and 10 dB less, respectively, than that with diploe [10]. For the aperture of a transducer within this high transmittance area, only the temple area, with a size of about 2 × 2 cm, is an effective acoustic window for transcranial sonication.

As previously mentioned, 0.5 MHz is a suitable ultrasound frequency for transcranial sonothrombolysis from the aspects of both thermal and mechanical effects, and several animal experiments have been reported [11], [12]. However, another frequency band is required for transcranial sonothrombolysis because a previous study reported that an over-dose of tPA can increase the risk of bleeding [5]–[7]; to suppress this bleeding risk, the ultrasound focal position and exposure time and the tPA dosage have to be optimized, and therefore, monitoring during therapy is required for the sonothrombolysis. The amount of blood flow at an infarction area is an effective monitoring parameter. The spatial distribution of blood flow in the brain is

Manuscript received September 20, 2009; accepted February 5, 2010. This work was supported in part by the Health and Labour Sciences Research Grants for Translational Research from the Japanese Ministry of Health, Labor and Welfare.

T. Azuma is with Hitachi Central Research Laboratory, Tokyo, Japan (e-mail: takashi.azuma.sa@hitachi.com).

M. Ogihara, J. Kubota, and A. Sasaki are with Hitachi Medical Corporation, Chiba, Japan.

S. Umemura is with Tohoku University, Sendai, Japan.

H. Furuhata is with the Medical Engineering Laboratory Research Center for Medical Science, Jikei University School of Medicine, Tokyo, Japan.

Digital Object Identifier 10.1109/TUFFC.2010.1534

visualized, and the velocity and temporal variation of the flow are also measured by TCD imaging. The frequency of 2 MHz is suitable for TCD imaging in view of the spatial resolution and transmittance of the skull.

The following two features are required for a transcranial sonothrombolysis system. First, ultrasound transmission frequencies of both 0.5 and 2 MHz need to be possible. Second, the total aperture size must be less than 2 × 2 cm. As the most reliable and widely used oscillator for imaging or therapeutic transducers among materials such as lead zirconate titanate (PZT) ceramics, poly vinylidene fluoride (PVDF) polymer, zinc oxide (ZnO) crystal, and so on, PZT ceramics are chosen because they have high electro-mechanical coupling coefficient and reliability of material. Because the maximum fractional bandwidth with PZT ceramic transducers is 70 to 80%, one PZT transducer cannot cover the frequency range of 0.5 to 2 MHz. In several previous works, dual-layer transducers were researched [13]–[15]. The frequency ratio of the overlaid array transducer proposed by de Fraguier is 1:10. The design concept by de Fraguier requires a large frequency separation between two frequency bands to drive each layer independently. Because of this, reducing the ratio of the two frequencies from 1:10 based on this design concept is difficult. The frequency ratio of the array transducer proposed by Hossack or Saitoh is 1:2. Because their design concept is based on coupling oscillation between dual layers, achieving short pulse transmission in the higher frequency band is essentially difficult. An alternative design method to achieve a dual-frequency sonothrombolysis array transducer that has a frequency ratio between 1:2 and 1:10 is required.

In this study, we used the following four steps: intuitive understanding based on 1-D analysis, optimization of the array structure using 2-D numerical simulation, fabrication, and evaluation. The 1-D model consisted of two PZT layers separated by an isolation layer. Reverberation of imaging pulses and transmittance of therapeutic ultrasound was analyzed in the 2-D simulation to optimize the acoustic impedance and thickness of the isolation layer by using the numerical simulation code PZFlex (Weidlinger Associates Inc., New York, NY) [16]. On the basis of this optimization, a prototype array transducer was fabricated, and its imaging and therapeutic performances were evaluated [17], [18].

II. Materials and Method

A. Concept Design of Dual-Frequency Array Using Frequency Selective Isolation Layer

Fig. 1 shows the structure of a dual-frequency array consisting of a 2-MHz TCD imaging array overlaid on a 0.5-MHz therapeutic array. If the 2-MHz TCD array is connected directly to the 0.5-MHz array, compressive oscillation of an element in one array will couple with one or several elements in the other array. Because this coupled

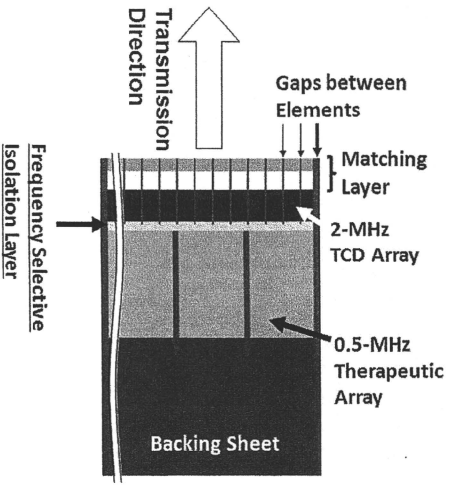

Fig. 1. Cross-sectional image of the concept design of the proposed overlaid transducer.

oscillation shifts the resonance frequencies of each array and causes crosstalk between elements, especially in the 2-MHz array, transmitting the expected ultrasound beam would be difficult. Therefore, we propose a new array transducer structure with a frequency selective isolation layer (FSIL) between the two arrays as shown in Fig. 1.

The FSIL is a thin polymer layer whose acoustic impedance is relatively small compared with that of PZT ceramics. The function of the FSIL is to isolate the imaging array from the therapy array at 2 MHz without disturbing the 0.5-MHz ultrasound transmitted for therapy. Because the ratios of the FSIL thickness to wavelengths in the FSIL at 0.5 and 2 MHz differ by four times, FSILs will have different functions at 0.5 and 2 MHz if the optimal thickness is chosen. Although an FSIL with a thickness of $\lambda/16$ at 0.5 MHz is almost transparent to therapeutic ultrasound propagation, a thickness of $\lambda/4$ at 2 MHz, which is equal to a thickness of $\lambda/16$ at 0.5 MHz, reflects the imaging ultrasound from the upper array effectively. This reflection should result in the TCD array being isolated from the therapeutic array by the FSIL.

The structure of a TCD array on a therapeutic array is more suitable than a structure in which the therapeutic array is on the TCD array for several reasons. First, to maintain the bandwidth of the transfer function of the TCD array (which corresponds to the spatial resolution of images obtained by the TCD array) it is desirable that the TCD array is in direct contact with the objects to be imaged, without any intervening layers. Second, there is no way to restore the reception efficiency of the TCD array, whereas the transmitted ultrasound power can be restored by increasing the driving electric voltage. The bandwidth

of the transfer function of the therapeutic array is not important because the therapeutic array transmits continuous waves and long burst waves, which have narrow bandwidths. Additionally, because the therapeutic array is used only for transmitting and is not used for receiving ultrasound, the gain of the therapeutic array is not as significant as that of the TCD array. On the basis on these considerations, the TCD array was mounted in the front of the therapeutic array.

One of the most important issues in this study is suppressing unwanted responses caused by reflected imaging pulses from the backside of the therapeutic array after propagation in the FSIL. Because a signal dynamic range reaching 100 dB is required for conventional ultrasound imaging, even a very small unwanted response in the echo signal can generate a visible artifact. To achieve the weakest possible unwanted response, the acoustic impedance and thickness of the FSIL must be optimized.

B. Optimization of the FSIL Using a 1-D Model

1) Three-Layer Model: To optimize the thickness and acoustic impedance of the FSIL, we calculated transmitted and reflected waves in a three-layer model consisting of the FSIL between two PZT ceramic arrays, as shown in Fig. 2. Assume that both PZT ceramic arrays have infinite thickness and the acoustic impedance of these layers is Z_1. The thickness and acoustic impedance of the FSIL are L and Z_0, respectively. We focused on a reflection wave and a transmission wave caused by incident wave $I(t)$ defined as

$$I(t) = \begin{cases} \sin \omega t & \text{when } 0 < t < \dfrac{2\pi}{\omega} \\ 0 & \text{otherwise.} \end{cases} \tag{1}$$

As shown in Fig. 2, R_1 is the reflection pulse reflected at boundary 1, R_2 is the reflection pulse after propagation in the FSIL and reflection at boundary 2, and R_3 is the reflection pulse after propagation in the FSIL with two reflections at boundary 2 and one reflection at boundary 1. Because the reflection wave $R(t)$ is the sum of these reflection pulses, the reflection wave can be calculated from

$$R(t) = -rI(t) + \sum_{k=1}^{\infty} t^2 r^{2k+1} I(t - 2kL/c), \tag{2}$$

where c is the velocity of ultrasound in the FSIL. The reflection coefficient r and the transmission coefficient t are given by

$$r = \frac{z_1 - z_0}{z_1 + z_0}, \quad t = \frac{2z_0}{z_1 + z_0}. \tag{3}$$

As shown in Fig. 2, T_1 is the transmission pulse without reflection at either of boundaries 1 or 2, T_2 is the transmission pulse after propagation in the FSIL and one reflection each at boundaries 1 and 2, and T_3 is the transmission pulse after propagation in the FSIL and two reflections each at boundaries 1 and 2. Because the transmission wave $T(t)$ is the sum of these transmission pulses, the transmission wave can be calculated from

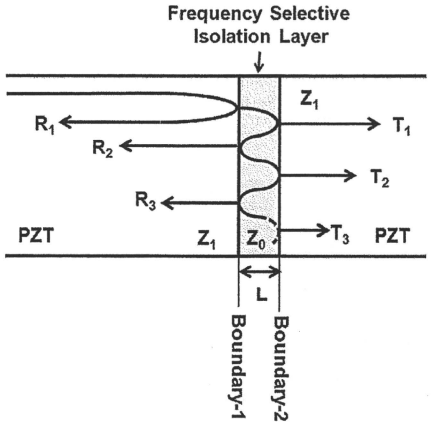

Fig. 2. Three-layer model consisting of a frequency selective isolation layer and two PZT layers.

$$T(t) = \sum_{k=1}^{\infty} t^2 r^{2k-2} I(t - (2k-1)L/c). \tag{4}$$

These peak-to-peak amplitudes of reflection and transmission waves were calculated with different acoustic impedances and thicknesses of the FSIL.

2) Reverberation Analysis: In this section, the estimation of reverberation caused by the reflection or transmission wave generated at the boundary between the FSIL and imaging array is described. The FSIL will be optimized on the basis of this estimation. To minimize the reverberation amplitude by optimizing the thickness and structure of the FSIL, we should consider the two following reverberation processes. One of the processes is caused by a reflection wave from the back part of the dual-layer array, and the other is caused by reflection waves from the front part of the dual-layer array. Details of the reverberation from the back part of the dual-layer array are as follows. If a pulse generated in the imaging array transmits through the FSIL, reflects at the backside of the therapeutic array, and transmits trough the FSIL again, this component will appear as a reverberation. This process is indicated as Pulse 1. The amplitude of this reverberation can be estimated by multiplying the square of the transmittance of the FSIL by the reflectivity at the back of the therapeutic array. As a typical case, when the acoustic impedance of the backing layer is 6 MRayl and that of the PZT ceramic is 40 MRayl, the reflection ratio is 0.74.

However, estimation of reverberation caused by reflection from the front part of the dual-layer array is more difficult because several possible reflections at several boundaries in the front part of the array will contribute to the reverberation. Two typical processes contribute to reverberation from the front part, indicated as Pulse 2a and Pulse 2b. Pulse 2a is from the reflection caused by mismatched propagation through the matching layers, and Pulse 2b is from the reflection occurring at the boundary between an imaging object and the acoustic lens.

In the case of Pulse 2a, we estimated the reflection amplitude using a pulse path tracking method. This pulse path tracking method based on a stochastic process only requires very simple computation. When one pulse reaches a boundary between two different materials, a random number N_r will be generated in the computation program. If N_r is less than the reflectivity of the boundary defined by two acoustic impedances, the particle will be reflected; if not, the particle will penetrate the boundary. This process will repeat until the particle reaches the region with acoustic impedance of Z_0 or Z_3. As a result of synthesis of many time-shifted waves based on each computed traveling distance, the waveforms of reflection or transmission will be calculated. After this pulse traveling process in the double matching layer is repeated 1000 times, a convergent reflected waveform is calculated. A reflectivity of 0.05 was obtained in this calculation. This series of calculations for multiple reflections in multilayer structure is called the pulse path tracking method in this paper.

In the case of Pulse 2b, a matching layer is ideally matched to both the imaging array and acoustic lens. As a result of this ideal matching, only the reflection at the boundary between the acoustic lens and imaging object will contribute to reverberation. For tissues, fat layers and typical tissues have acoustic impedances of 1.3 and 1.5 MRayl, respectively. Because the acoustic impedance of tissue contacting the acoustic lens is not constant, matching the acoustic impedance of the lens with that of the contacting tissue is difficult. To minimize the reflectivity between the lens and the contacting tissue, the acoustic impedance of the lens was optimized to be 1.4 MRayl for that of the contacting tissue ranging from 1.3 to 1.5 MRayl. This results in reflectivity between the lens and tissue surface being 0.06.

In our reverberation estimation, we use the two previously mentioned typical reflectivities to estimate the contribution from the front part of an array to reverberation. By using the combined 1-D reverberation simulation, we optimized the acoustic impedance and thickness of the FSIL.

C. Optimization of FSIL Using the 2-D Finite Element Method

The thickness, density, and longitudinal velocity of the two matching layers and the PZT ceramics in the TCD array are defined based on the previously optimized parameters when the TCD array oscillates independently in conventional-structure array transducers. The thickness of the therapeutic array is defined based on the resonance frequency of the PZT ceramics. In this study, we only optimize the acoustic impedance and thickness of the FSIL. The acoustic impedance is adjusted by changing the density, because the longitudinal velocity is constant. The thickness of the FSIL is investigated around the quarter length of the wavelength at 2 MHz, which is so thin that the absorption coefficients of the FSIL are not expected to affect the results. On the basis of this consideration, the absorption coefficient of the FSIL is fixed at a value of a typical polymer.

The optimization sequence in this study is as follows.

1) Model the array structure.
2) Analyze oscillation of each TCD and therapeutic array.
3) Analyze crosstalk between elements in the TCD array.

Suppression of crosstalk is an important function of the FSIL for the several reasons. The width of a PZT element in the therapeutic array is four times that in the TCD array, and four elements are fabricated on one therapeutic element. If isolation achieved by the FSIL is not sufficient, the four elements fabricated on the therapeutic element will oscillate with coupling between all of the elements. Because this coupled oscillation causes crosstalk, controlling the beamforming becomes difficult.

4) Search for optimal thickness and acoustic impedance of FSIL.

This optimization was performed based on simulation results of amplitudes of unwanted responses in transfer functions of TCD arrays.

Fig. 1 shows a simulation model in a numerical simulator, PZFlex. PZFlex solves the piezoelectric coupled wave equation on the basis of a finite element method. The grid size was 15 μm, and absorbing boundary conditions were used. The actual width of an element in the elevation axis was around 10 mm. Because this width is about 30 times larger than the element widths in the other two axes, we used 2-D simulation.

D. Prototype Fabrication and Evaluation

We fabricated a prototype dual-frequency array transducer on the basis of the optimization results. Because the optimal thickness of the FSIL is thinner than the limit applied in actual fabrication processes, we chose 3 MRayl as the acoustic impedance and 100 μm as the thickness. The fabrication process was as follows.

1) A therapeutic PZT ceramic array was connected to a flexible printed circuit sheet and mounted on a backing block.
2) The therapeutic PZT ceramic array was diced to fabricate a therapeutic array.

3) An FSIL sheet was bonded to the therapeutic array.
4) A PZT ceramic array for TCD, connected to a flexible printed circuit sheet, was mounted on the FSIL.
5) The PZT ceramic array for TCD was diced to fabricate a TCD array. The TCD elements are separated from the adjacent elements by complete kerf cut. However, multiple TCD elements were mounted on each therapeutic element through the FSIL. Because this structure has a possible practical problem of a crosstalk between TCD elements via the therapeutic element, this problem will evaluated quantitatively in the next section.
6) An acoustic lens was mounted on the TCD array.

Round-trip responses of the prototype array were measured by a pulser-receiver (5900PR, Panametrics, Waltham, MA), and the data were acquired by a digital oscilloscope (TDS3034, Tektronix, Beaverton, OR). The reflector, consisting of an aluminum plate, was placed 4 cm from the transducers. Phantom images and human TCD images obtained by the prototype array with an ultrasound scanner (EUB-8500, Hitachi Medical Co., Chiba, Japan) were evaluated. An acoustic pressure beam pattern generated from the therapeutic array in the fabricated transducer was measured with a calibrated hydrophone (HGL-0200, Onda Corp., Sunnyvale, CA).

III. Results

A. Optimization of FSIL Using 1-D Model

1) Optimization of FSIL Using Three-Layer Model: Figs. 3 and 4 show the simulation results of peak-to-peak amplitude mapping of transmission and reflection waves by calculating pulse propagations in the three-layer model in a decibel scale. Pulse durations are different in these two mappings. A one-cycle sinusoidal wave and a nine-cycle sinusoidal wave were used as incident waves in Figs. 3 and 4, respectively. The horizontal axis is the thickness of the FSIL, which is normalized by the wavelength in the FSIL at 2 MHz. The vertical axis indicates the acoustic impedance of the FSIL, which is normalized by that of the PZT ceramic. In both long burst and short pulse conditions, the magnitudes of the transmission waves increased and that of the reflection waves decreased as the impedance of the FSIL increased. The dependences of the reflection and transmission magnitudes on the thickness changed periodically. They have minimum values at the quarter wavelength when there were nine cycles of a sinusoidal wave. In contrast, the magnitude of the transmission had the minimum value when the isolation thickness-to-wavelength ratio was between 1/6 and 1/7. The magnitude of reflection was almost constant except when the thickness-to-wavelength ratio was around 1/10.

Simulation results of peak-to-peak amplitude mapping of transmission waves by calculating pulse propagations

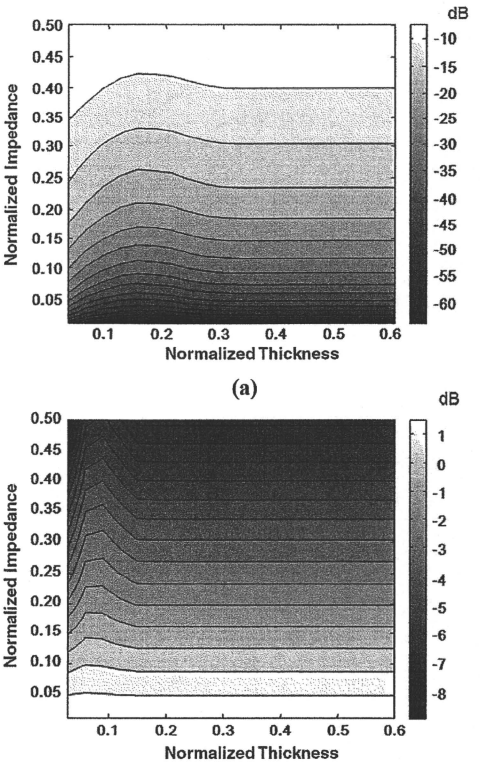

Fig. 3. Simulation results of peak-to-peak amplitude mapping of transmission (a) and reflection (b) waves by calculating pulse propagation in the three-layer model in dB scale with a one-cycle sinusoidal wave. The horizontal axis is thickness of the frequency selective isolation layer (FSIL), which is normalized by the wavelength in the FSIL at 2 MHz. The vertical axis is the acoustic impedance of the FSIL, which is normalized by that of the PZT ceramic.

in the three-layer models showed that the magnitude of the transmission waves increased as the impedance of the FSIL increased and the thickness of the FSIL decreased.

2) Reverberation Analysis: Reverberation amplitudes estimated with the three-layer model are plotted in Fig. 5. The solid line in Fig. 5 is the estimated amplitude of reverberation from the back part of the transducer based on the transmission ratio of the FSIL as shown in Fig. 3(a) and the reflection ratio of 0.74. The dashed line is the estimated amplitude of reverberation from the front part of the transducer based on the reflection ratio of the FSIL as shown in Fig. 3(b) and on the reflection ratio at the matching layer (0.05). The dotted line is that based on the reflection ratio of the FSIL as shown in Fig. 3(b)